

Absolute measurement of quadratic nonlinearities from phase-matched second-harmonic generation in a single KTP crystal cut as a sphere

B. Boulanger, J. P. Fève, and G. Marnier

Laboratoire de Physique de l'Université de Bourgogne, Faculté des Sciences et Techniques, B.P. 400, 21011 Dijon Cedex, France

C. Bonnin and P. Villeval

Cristal Laser SA, B.P. 44, 54230 Chaligny, France

J. J. Zondy

Laboratoire Primaire du Temps et des Fréquences, Observatoire de Paris, 61 avenue de l'Observatoire, 75014 Paris, France

Received September 27 1996; revised manuscript received December 24, 1996

We determine within an accuracy of $\sim 10\%$ the absolute magnitude of the quadratic effective coefficients of types I and II phase-matched second-harmonic generation from conversion efficiency measurements in a single nonlinear crystal cut as a sphere. The agreement is good with measurements performed in thin parallelepipedal samples. The material studied is KTiOPO_4 , for which improved Sellmeier equations are given. © 1997 Optical Society of America [S0740-3224(97)03308-7]

1. INTRODUCTION

Knowledge of the absolute magnitude and the relative sign of the independent coefficients of the second-order electric susceptibility tensor $d^{(2)}_{ij} [= 1/2\chi^{(2)}_{ij}]$ is of prime importance for qualification of a new nonlinear crystal and also for fundamental engineering of nonlinear-optical materials. However, measurement of quadratic nonlinear coefficients still presents a problem: There are often disparities between published values relative to the same crystal, even if the crystal, such as KTiOPO_4 (KTP), has long been commonly used in efficient devices.¹⁻⁴

The disagreement of various absolute magnitudes sometimes arises from the fluctuation of the crystal quality, but it is often the result of the measurement technique. All the measurement methods are based on the powers of incident and generated beams. Two techniques use non-phase-matched second-harmonic generation (SHG): The harmonic signal oscillates as a consequence of the rotation of a parallelepiped (Maker-Fringe technique)⁵ or of the translation of a prism (prism technique).⁶ SHG is also used with a parallelepipedal crystal cut in a phase-matching direction that leads to higher conversion efficiency than the non-phase-matched interactions.⁷ Another technique uses parametric fluorescence.⁴

The volume of material required for performing the essential measurements for accurate determination of the basic optical properties of a new nonlinear crystal at an early stage of its growth is important. Among these properties are its Sellmeier's equations, phase-matching

directions and the associated effective coefficients, and the absolute magnitude and the relative sign of the nonlinear coefficients in the transparency range. Determination of Sellmeier's coefficients requires two or three millimetric samples cut as a prism (angle of minimum deviation) or as a strip (total reflection angle). The best accuracy is $\sim 10^{-4}$ in the visible range and 10^{-3} in the infrared range; these values are not sufficient to permit us to calculate a phase-matching direction successfully. It is then necessary to rotate the crystal cut in the calculated phase-matching direction, or, when the rotation is not sufficient, to cut several samples in different directions to measure the phase-matching direction. New methods are based on the use of spheroidal⁸ or spherical⁹ geometries, which provide accurate phase-matching angles. One millimetric sample permits the determination of any phase-matching direction with the orientation symmetry as the only initial datum. That kind of measurement permits improvement of the Sellmeier equations obtained by the methods described above. The magnitude and the relative sign of the independent $d^{(2)}$ coefficients are often measured by non-phase-matched SHG, which requires two or three millimetric parallelepipedal crystals. The phase-matched SHG method is more accurate but requires study of as many directions as there are independent tensor coefficients, which one usually does with several strips.

We show here that measurement of the phase-matched SHG conversion efficiency in a sphere can lead to the determination of the absolute magnitude of the effective co-

efficient d_{eff} of the subject phase-matching direction with an accuracy of $\sim 10\%$. The best accuracy that we can achieve in a thin strip is $\sim 5\%$.³ As for the classical methods using parallelepipeds, it is necessary to know the refractive indices to be able to calculate the theoretical SHG conversion efficiency.^{10,11} However, we are interested in a sphere because for a sphere it is possible to measure the SHG conversion efficiency in all the desired phase-matching directions. Then a judicious choice of several types I and II phase-matching directions permits the determination of the absolute magnitude of the independent $d_{ij}^{(2)}$ coefficients, with only one crystal. We showed previously that the sphere method is suitable for determination of the relative sign of the independent $d^{(2)}$ coefficients; we established, for the first time to our knowledge, that d_{15} , d_{24} , and d_{33} of KTP have the same sign.³ We used halide flux-grown KTP crystals,¹² for which we propose accurate Sellmeier equations from measurements of the optical axis and the phase-matching angles.^{11,13-17}

2. REFRACTION

We consider a spherical anisotropic medium. Any direction of propagation, with the spherical coordinates (θ, ϕ) , is characterized by two refractive indices, $n^+(\theta, \phi)$ and $n^-(\theta, \phi)$, which correspond to the two polarization eigenmodes. n^+ and n^- are described in Appendix A.

The sphere is illuminated with a Gaussian laser beam. Then, according to the $ABCD$ ray matrix of the sphere, i.e.,

$$\begin{bmatrix} 1 & 0 \\ \frac{1-n}{nR} & \frac{1}{n} \end{bmatrix},$$

where R is the sphere's radius, the refracted beam parameters (w_o', d') , defined in Fig. 1, are related to the incident beam parameters (w_o, d) by the following equations¹⁸:

$$w_o' = \frac{w_o}{n\sqrt{E^2 + F^2}}, \quad d' = \frac{-dE - F\left(\frac{\pi w_o^2}{\lambda}\right)}{(E^2 + F^2)},$$

$$E = \frac{1}{n} + \frac{1-n}{nR}d, \quad F = \frac{1-n}{nR} \frac{\pi w_o^2}{\lambda}, \quad (1)$$

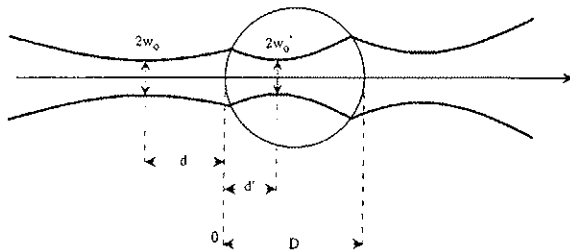


Fig. 1. Incident (w_o, d) and refracted (w_o', d') Gaussian beam parameters. D is the sphere diameter. The origin of the d, d' axis is taken as the entrance surface of the sphere.

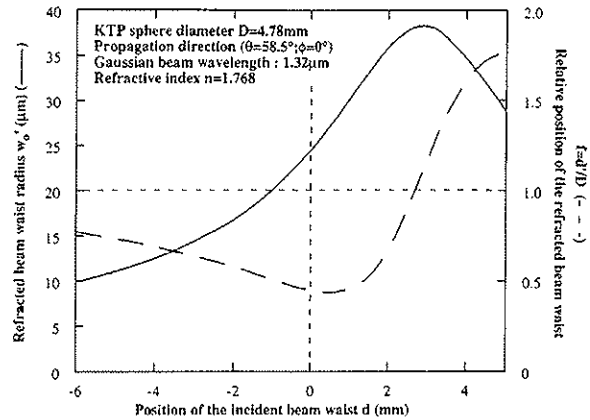


Fig. 2. Refracted Gaussian beam parameters in the sphere (w_o', d') calculated for incident beam radius $w_o = 31.6 \mu\text{m}$. $d = 0$ corresponds to an incident beam waist located at the sphere entrance. The focusing parameter is $f = d'/D$, so the refracted beam waist is at the sphere entrance for $f = 0$ and at the exit for $f = 1$.

where w_o is the radius of the incident beam waist, d is the distance between the incident waist and the sphere entrance, $n = n^+$ or $n = n^-$ is the refractive index, and λ is the wavelength. The distance d' is usually expressed in terms of the focusing parameter, $f = d'/D$, where D is the sphere's diameter.

We take the example of a direction in KTP at $(\theta = 58.5^\circ, \phi = 0^\circ)$. This direction is assumed in parts of Sections 3 and 4 below. In this direction the refractive indices of the eigenmodes are $n^+ = 1.7962$ and $n^- = 1.7406$. The corresponding refracted beam parameters are $w_o'^+ = 18.63 \mu\text{m}$, $w_o'^- = 19.27 \mu\text{m}$, $d'^+ = 2.58 \text{ mm}$, and $d'^- = 2.56 \text{ mm}$, corresponding to $f^+ = 0.540$ and $f^- = 0.536$ calculated from relations (1) with $w_o = 31.6 \mu\text{m}$, $d = -1.5 \text{ mm}$, $\lambda = 1.32 \mu\text{m}$, and $R = 2.39 \text{ mm}$. It appears that the eigenmode parameters are very close together, which is always the case for the typical situations that we study. It is then a reasonable approximation to consider that the two eigenmodes are identically refracted in the sphere, with the parameters w_o' and d' calculated from the average value of n^+ and n^- , which for the situation previously considered yields $n = 1.768$, $w_o' = 18.95 \mu\text{m}$, and $f = 0.538$. w_o' and f are plotted in Fig. 2 as a function of d .

3. PHASE-MATCHED SHG

A. Gaussian Model

Phase matching is suitable for the determination of nonlinear coefficients because it provides high SHG conversion efficiency. It is then possible to use a cw fundamental beam and get a harmonic signal that can easily be detected. This possibility is of prime interest because the temporal shape of a pulsed beam often leads to uncertainties in the calculation of the instantaneous power.

If the incident fundamental power is sufficiently low to validate the undepleted-pump approximation, it is possible to make an accurate model of SHG, even if there is angular walk-off and if the crystal length is larger than

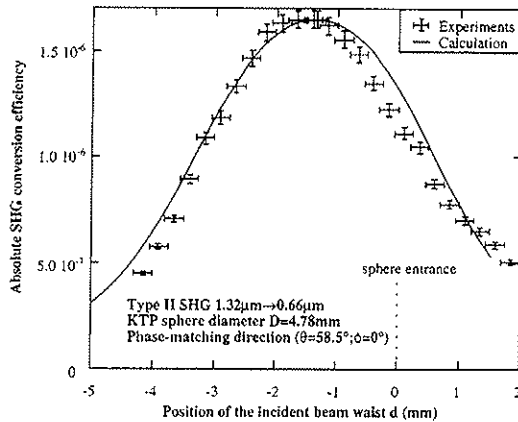


Fig. 3. Type II phase-matched SHG conversion efficiency at the sphere exit as a function of the focusing conditions for an incident power of 648 ± 30 mW at $1.32 \mu\text{m}$.

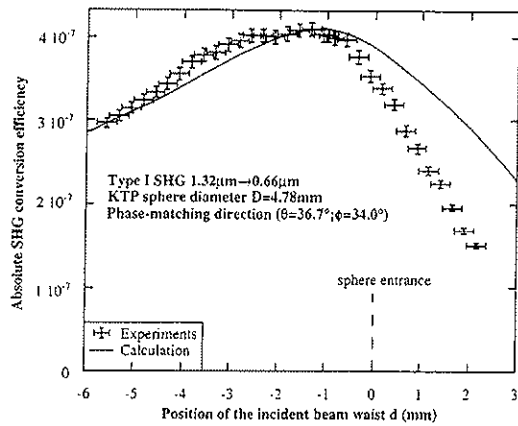


Fig. 4. Type I phase-matched SHG conversion efficiency at the sphere exit as a function of the focusing conditions for an incident power of 613 ± 30 mW at $1.32 \mu\text{m}$.

the Rayleigh length inside the crystal. In that case the SHG conversion efficiency for TEM_{00} Gaussian beams is expressed as¹⁰

$$\eta_{\text{SHG}}(L) = \frac{P^{2\omega}(L)}{P^{\omega}(0)} = \text{CLP}^{\omega}(0) \frac{h(L, \omega_o', \rho, f, \Delta k)}{\cos^2 \rho_{2\omega}}, \quad (2)$$

where all parameters are detailed in Appendix B. In this model the two fundamental beams are assumed to be refracted with the same beam radius and the same Rayleigh length. For type I this is so because the two fundamental beams have the same polarization. For type II the model is an approximation because the two refractive indices n^+ and n^- at the fundamental wavelength are required. In fact, for typical values of birefringence $n^+ - n^-$, the associated refracted parameters $(\omega_o', d')^+$ and $(\omega_o', d')^-$ are close; thus it is possible to consider an average Rayleigh length $z_o' = \pi(n_o^+ + n_o^-)\omega_o'^2/2\lambda_o$ for the calculation of type II SHG conversion efficiency. Note that this approximation is consistent with those made for the calculation of refraction in the sphere. The validity of this model has been proved

by systematic experiments using parallelepipedal KTP crystals for different lengths and beam geometries.¹⁹ The two kinds of experiment described below indicate that the Gaussian model is also valid for phase-matched SHG in a sphere.

B. Focusing Conditions

In Figs. 3 and 4 are plotted the measured and calculated $1.32\text{-}\mu\text{m}$ SHG conversion efficiencies as a function of d , the distance between the incident beam waist and the sphere entrance, for the two phase-matching directions of type I and II of highest efficiency.

Distance d is measured by a micrometric translation associated with a sighting telescope. The radius of the incident beam is $w_o = 31.6 \mu\text{m}$, measured by an accurate method that we developed previously.²⁰

The effective coefficient d_{eff} used for the calculated curve is normalized to the measured curve at the optimum of efficiency. The d evolution is then calculated from Eqs. (2) and (B1) and (B2) below at the optimum mismatch and with the refracted beam parameters obtained from Eqs. (1). The corresponding refractive indices and walk-off angles, which are given in Table 1, arise from the new Sellmeier equations¹⁴:

$$n_x^2(\lambda) = 2.1239 + \frac{0.14274\lambda^2}{\lambda^2 - 18.477} + \frac{0.87370\lambda^2}{\lambda^2 - 0.045906},$$

$$n_y^2(\lambda) = 2.0649 + \frac{0.15529\lambda^2}{\lambda^2 - 19.373} + \frac{0.95463\lambda^2}{\lambda^2 - 0.045505},$$

$$n_z^2(\lambda) = 1.6539 + \frac{0.34767\lambda^2}{\lambda^2 - 29.378} + \frac{1.6482\lambda^2}{\lambda^2 - 0.038825}. \quad (3)$$

We have established Eqs. (3) from optical axis and phase-matching direction angles between 0.5 and $2.5 \mu\text{m}$.^{11,13-17} These measurements provide an accurate relative magnitude of the principal refractive indices. We then obtained the absolute value by taking n_x and n_z equal to the values given at $1.32 \mu\text{m}$ in Ref. 21.

The agreement between experiment and calculation is very good for type II over the entire d range considered. For type I the agreement is good between -6 mm and 0 ; we have no satisfactory explanation for the discrepancy over the positive range.

C. Angular Bandwidths

Another good way to illustrate the validity of the Gaussian model for the sphere is to consider the angular variation of the SHG conversion efficiency around a phase-matching direction. Figures 5 and 6 concern $1.064\text{-}\mu\text{m}$ type II SHG in the a - b and b - c planes of KTP. The calculation is performed from Eqs. (1), (2), (B1), and (B2), with the refractive indices and walk-off angles calculated from Eqs. (3) and given in Table 1. The experimental and calculated curves are normalized. This study is interesting because it shows that there is a good agreement-

Table 1. Calculated Refractive Indices (n_i) Total Transmission Coefficient (T), Walk-Off Angle (ρ), Field Factors (F_{ij}), and Aperture Functions (h_{opt}) Corresponding to the Phase-Matching Directions Studied (θ, ϕ)^a

Parameters Used for Calculations	For Type II SHG (1.32 μm \rightarrow 0.66 μm)		For Type I SHG (1.32 \rightarrow 0.66 μm)	For Type II SHG (1.064 μm \rightarrow 0.532 μm)	
	$\theta = 58.5^\circ, \phi = 0^\circ$	$\theta = 49.4^\circ, \phi = 90^\circ$	$\theta = 36.7^\circ, \phi = 34^\circ$	$\theta = 90^\circ, \phi = 23.1^\circ$	$\theta = 68.3^\circ, \phi = 90^\circ$
n_1^ω	1.7406	1.7339	1.7654	1.7453	1.7393
n_2^ω	1.7962	1.7858	1.7654	1.8294	1.8185
$n_3^{2\omega}$	1.7684	1.7599	1.7654	1.7873	1.7789
$T_3^{2\omega} T_1^\omega T_2^\omega = T$	0.7862	0.7894	0.7873	0.7791	0.7823
ρ ($^\circ$)	2.57	2.59	2.12	0.23	1.81
F_{15}	0	0.7286	0.4446	0.1789	0.9196
F_{24}	0.8282	0	-0.4658	0.8211	0
F_{31}	0	0	0.02315	0	0
F_{32}	0	0	0.01700	0	0
F_{33}	0	0	0.01819	0	0
h_{opt} :	0.0142	0.0140	0.1843	0.550	0.0163
sphere, ($D = 4.78$ mm)					
Parallelepiped	0.04898 ($L = 0.492$ mm)	0.04909 ($L = 0.492$ mm)	0.09284 ($L = 0.930$ mm)	0.07345 ($L = 0.891$ mm)	0.05772 ($L = 0.891$ mm)

^a D is the sphere diameter and L is the length of parallelepipeds.

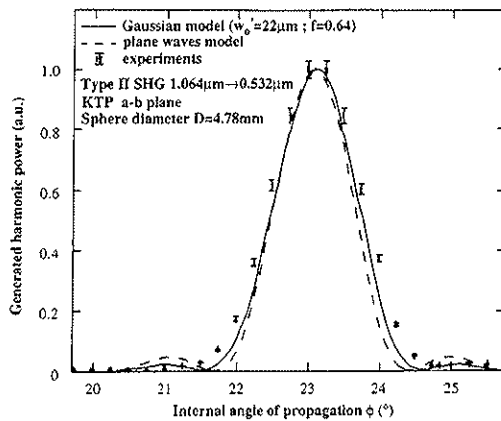


Fig. 5. Angular variation of type II SHG conversion efficiency near a phase-matching direction with a walk-off angle of 0.23° .

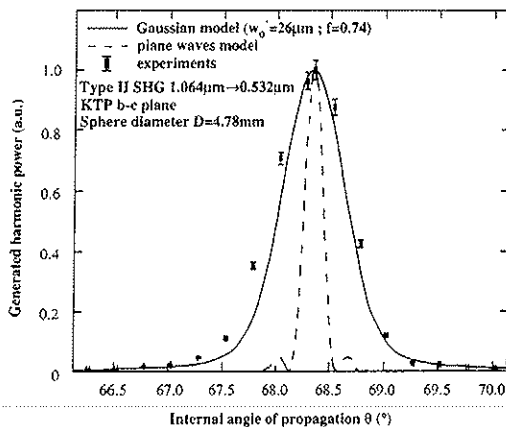


Fig. 6. Angular variation of type II SHG conversion efficiency near a phase-matching direction with a walk-off angle of 1.81° .

between experiment and calculation over a broad range of walk-off angles, i.e., from 0.23° to 1.81° . We also give the calculation performed with the plane-wave model.²² The discrepancy is large in the b - c plane, where the walk-off angle is high, indicating that the angular bandwidth is sensitive to the beam geometry and to the walk-off angle.

4. MEASUREMENT OF THE NONLINEAR COEFFICIENT

The studies described in Sections 2 and 3 indicate that determination of the absolute magnitude of the effective coefficient d_{eff} in any phase-matching direction is possible from a sphere experiment modeled by the $ABCD$ ray matrix law and the SHG Gaussian model. This is confirmed by the relative effective coefficients measured in a sphere and a parallelepiped for five different phase-matching directions. The corresponding ratios are given in Table 2, according to the measured relative powers and by use of Eq. (2); all the calculated parameters are given in Table 1. The agreement between the sphere and the parallelepiped is satisfying for type II experiments. For type I the sphere measurements led to an effective coefficient a bit smaller than the value obtained with a parallelepiped. This discrepancy could be connected to the existing one for the SHG efficiency experiments as a function of d in the positive range, as shown in Fig. 4.

In Table 3 we give the absolute fundamental and harmonic powers of the three SHG experiments at $1.32 \mu\text{m}$ in spheres and parallelepipeds at the optimum of conversion efficiency. The absolute values of the corresponding effective coefficients, listed in Table 4, are determined from these data and by use of Eq. (2) with the calculated parameters of Table 1. The absolute values of d_{15} , d_{24} , and d_{33} are then determined from the following equations³:

Table 2. Comparison of Effective Coefficients Determined by Sphere and Parallelepiped Experiments, $d_{\text{eff}}^{\text{sphere}}/d_{\text{eff}}^{\text{parallelepiped}}$

Type II, 0.66 μm		Type I, 0.66 μm	Type II, 0.532 μm	
$\theta = 58.5^\circ, \phi = 0^\circ$	$\theta = 49.4^\circ, \phi = 90^\circ$	$\theta = 36.7^\circ, \phi = 34^\circ$	$\theta = 90^\circ, \phi = 23.1^\circ$	$\theta = 68.3^\circ, \phi = 90^\circ$
1.05 ± 0.15	1.03 ± 0.15	0.79 ± 0.12	1.04 ± 0.09	1.05 ± 0.08

Table 3. Fundamental (P^ω) and Harmonic ($P^{2\omega}$) Powers of Three 1.32- μm SHG Experiments Performed in Spheres and Parallelepipeds

Power	Parallelepiped			Sphere		
	Type II		Type I	Type II		Type I
	$\theta = 58.5^\circ, \phi = 0^\circ$	$\theta = 49.4^\circ, \phi = 90^\circ$	($\theta = 36.7^\circ, \phi = 34^\circ$)	$\theta = 58.5^\circ, \phi = 0^\circ$	$\theta = 49.4^\circ, \phi = 90^\circ$	($\theta = 36.7^\circ, \phi = 34^\circ$)
P^ω (mW)	557 ± 30	551 ± 30	613 ± 30	518 ± 24	533 ± 24	576 ± 30
$P^{2\omega}$ (nW)	372 ± 14	72.9 ± 3.0	42.2 ± 1.9	994 ± 60	204 ± 8	236 ± 11

Table 4. Absolute Effective Coefficients and d_{ij} Coefficients Measured from Sphere and Parallelepiped Experiments

$d^{(2)}$ Coefficients at 0.66 μm (pm/V)	Absolute Coefficients		
	From 1.32- μm SHG Experiments in Spheres	From 1.32- μm SHG Experiments in Parallelepipeds	From Miller's Rule According to 1.064- μm SHG in Parallelepipeds ^a
$d_{\text{eff}}^{\text{II}}(\theta = 58.5^\circ, \phi = 0^\circ)$	2.05 ± 0.16	1.96 ± 0.14	2.08 ± 0.11
$d_{\text{eff}}^{\text{II}}(\theta = 49.4^\circ, \phi = 90^\circ)$	0.90 ± 0.07	0.87 ± 0.06	0.97 ± 0.05
$d_{\text{eff}}^{\text{II}}(\theta = 36.7^\circ, \phi = 34^\circ)$	-0.249 ± 0.019	-0.315 ± 0.022	-0.322 ± 0.016
d_{15}	1.24 ± 0.10	1.19 ± 0.08	1.33 ± 0.07
d_{24}	2.47 ± 0.19	2.37 ± 0.17	2.51 ± 0.13
d_{33}	15.4 ± 8.3	10.6 ± 7.5	10.0 ± 5.9

^aThe values deduced from Miller's rule come from Ref. 3.

$$d_{24} = d_{\text{eff}a-c}^{\text{II}}/F_{24a-c}^{\text{II}},$$

$$d_{15} = d_{\text{eff}b-c}^{\text{II}}/F_{15b-c}^{\text{II}},$$

$$d_{33} = \frac{d_{\text{eff}}^{\text{I}} - d_{15}(F_{15}^{\text{I}} + F_{31}^{\text{I}}) - d_{24}(F_{24}^{\text{I}} + F_{32}^{\text{I}})}{F_{33}^{\text{I}}}. \quad (4)$$

The expressions for the various field factors F_{ij} are given in Appendix C. The indices $a-c$ and $b-c$ refer to the principal planes according to the convention given in Appendix A. The coefficient d_{33} is calculated from $d_{\text{eff}}^{\text{I}}$, d_{15} , and d_{24} , assuming a Kleinmann approximation, i.e., $d_{15} = d_{31}$ and $d_{24} = d_{32}$. All these coefficients have the same sign, as was clearly established in a previous paper.³

Because of the values of d_{eff} , the agreement between the sphere and the parallelepiped is good for d_{15} and d_{24} , but is unsatisfactory for d_{33} .

Furthermore, the accuracy of d_{33} is not good because it includes not only the accuracy of $d_{\text{eff}}^{\text{I}}$ but also those of d_{15} and d_{24} ; this is true especially when the magnitude of F_{33}^{I} is very small. This situation is inherent in type I KTP, for which F_{31}^{I} , F_{32}^{I} , and F_{33}^{I} are less than 1 order of magnitude smaller than F_{15}^{I} and F_{24}^{I} because of the quasi-

uniaxial character of KTP, i.e., $(n_y - n_x)/(n_z - n_{x,y}) \approx 0.1$. However, the measured magnitude of d_{33} is significant, especially because the agreement is good between the parallelepiped experiments at 1.064 μm (Ref. 3) and 1.32 μm according to Miller's rule, as is shown in Table 4. Note that we had underestimated the uncertainty of d_{33} in our previous paper.³

5. CONCLUSION

We have shown that quadratic nonlinear coefficients can be determined with an accuracy of $\sim 10\%$ from phase-matched SHG conversion efficiency measurements performed in a millimetric single crystal cut as a sphere. These values are in good agreement with those determined with parallelepipeds for type II SHG. It is less satisfactory for type I, but it is difficult now to improve the model to correct the effective coefficient shift. Doing so would require other measurements with different beam geometries and sphere diameters and with other crystals. These first results of absolute measurements of $d^{(2)}$ coefficients are encouraging. We could attempt to generalize the use of the spherical geometry for non-phase-matched SHG and parametric fluorescence. But a limitation will probably exist because of the weak effi-

ciency of these interactions: The generation of a measurable signal requires high intensities, which could damage the sphere.

APPENDIX A

n^+ and n^- are the two solutions of Fresnel's equation:

$$n^{\pm} = \left[\frac{2}{-B \mp (B^2 - 4C)^{1/2}} \right]^{1/2},$$

$$B = -u_x^2(b+c) - u_y^2(a+c) - u_z^2(a+b),$$

$$C = u_x^2bc + u_y^2ac + u_z^2ab,$$

$$a = n_x^{-2}(\omega), \quad b = n_y^{-2}(\omega), \quad c = n_z^{-2}(\omega), \tag{A1}$$

where $n_x(\omega)$, $n_y(\omega)$, and $n_z(\omega)$ are the principal refractive indices of the index ellipsoid at the circular frequency ω in the optical frame (x, y, z). In the case of KTP, this frame corresponds to the crystallographic frame (a, b, c), where c is the binary axis. (u_x, u_y, u_z) are the Cartesian coordinates of the unit wave vector \hat{u} related to the spherical coordinates (θ, ϕ) by

$$u_x = \cos \phi \sin \theta, \quad u_y = \sin \phi \sin \theta, \quad u_z = \cos \theta. \tag{A2}$$

APPENDIX B

The parameters of formula (2) for the calculation of the SHG conversion efficiency with Gaussian beams are

$$C = 5.95 \times 10^{-2} \frac{2N - 1}{N} \frac{d_{\text{eff}}^2}{\lambda_\omega^3} \frac{n_1^\omega + n_2^\omega}{2} \frac{T_3^{2\omega} T_1^\omega T_2^\omega}{n_3^{2\omega} n_1^\omega n_2^\omega}$$

(per watt meter). (B1)

N is the number of independently oscillating modes at the fundamental wavelength. Every longitudinal mode at the harmonic pulsation can be generated by many combinations of two fundamental modes. The $(2N - 1)/N$ statistical factor takes into account the fluctuations between these longitudinal modes. $P^\omega(0)$ is the total incident fundamental power (in watts); $P_1^\omega(0) = P_2^\omega(0) = P^\omega(0)/2$. w_0' (meters) is the beam radius, which is assumed to be the same for the two fundamental beams inside the crystal, that of the harmonic beam being $w_0'/\sqrt{2}$. L (meters) is the crystal length in the direction of propagation. $n_3^{2\omega}$, n_1^ω , and n_2^ω are the refractive indices at the harmonic and fundamental wavelengths $\lambda_{2\omega}$ and λ_ω (micrometers). For the phase-matching case, $n_3^{2\omega} = n^-(2\omega)$, $n_1^\omega = n_2^\omega = n^-(\omega)$ for type I and $n_1^\omega = n^+(\omega) \neq n_2^\omega = n^-(\omega)$ for type II. $T_3^{2\omega}$, T_1^ω , and T_2^ω are the transmission coefficients given by $T_i = 4n_i/(n_i + 1)^2$. d_{eff} (picometers per volt) ($=1/2\chi_{\text{eff}}$) is the effective coefficient; $d_{\text{eff}} = F^{(2)}d^{(2)}$ is the tensorial contraction of $d^{(2)}$ (picometers per volt) and of the field tensor $F^{(2)}$ in the direction of propagation considered. The field tensor is defined as the tensorial product of the three interacting unit electric field vectors.²³ $\rho_{2\omega}$ is the harmonic double-refraction angle. (The field tensors and double-refraction angles are defined in Appendix C.) $h(L, w_0', \rho, f, \Delta k)$ is the aperture function, given by¹⁰

$$h(L, w_0', \rho, f, \Delta k) = \frac{2z_0' \sqrt{\pi}}{L} \int_{-z}^{+z} |H(a)|^2 \times \exp(-4a^2) da,$$

with

$$H(a) = \frac{1}{\sqrt{2\pi}} \int_{-fL/z_0'}^{L(1-f)/z_0'} \frac{d\tau}{1+i\tau} \times \exp\left[-\gamma^2 \left(\tau + \frac{fL}{z_0'}\right)^2 - i\sigma\tau\right]. \tag{B2}$$

For type I, $\gamma = 0$, $\sigma = \Delta k z_0' + 4(\rho z_0'/w_0')a$; for type II, $\gamma = \rho z_0'/w_0' \sqrt{2}$, $\sigma = \Delta k z_0' + 2(\rho z_0'/w_0')a$. The walk-off angle ρ is defined by the maximum difference between the angles of double refraction of the three waves in the direction considered. The focusing parameter $f = d'/L$ gives the position of the beam waist inside the crystal, as defined above. Δk is a mismatch parameter, which takes into account the distribution of the mismatch, including collinear and noncollinear interactions, that is due to the divergence of the beams.

APPENDIX C

The field factors are expressed as

$$F_{15}^I(\theta, \phi) = 2e_x^-(2\omega, \theta, \phi)e_x^+(\omega, \theta, \phi)e_z^+(\omega, \theta, \phi),$$

$$F_{24}^I(\theta, \phi) = 2e_y^-(2\omega, \theta, \phi)e_y^+(\omega, \theta, \phi)e_z^+(\omega, \theta, \phi),$$

$$F_{31}^I(\theta, \phi) = e_z^-(2\omega, \theta, \phi)[e_x^+(\omega, \theta, \phi)]^2,$$

$$F_{32}^I(\theta, \phi) = e_z^-(2\omega, \theta, \phi)[e_y^+(\omega, \theta, \phi)]^2,$$

$$F_{33}^I(\theta, \phi) = e_z^-(2\omega, \theta, \phi)[e_z^+(\omega, \theta, \phi)]^2,$$

$$F_{15}^{II}(\theta, \phi) = e_x^-(2\omega, \theta, \phi)[e_x^+(\omega, \theta, \phi)e_z^-(\omega, \theta, \phi) + e_x^-(\omega, \theta, \phi)e_z^+(\omega, \theta, \phi)],$$

$$F_{24}^{II}(\theta, \phi) = e_y^-(2\omega, \theta, \phi)[e_y^+(\omega, \theta, \phi)e_z^-(\omega, \theta, \phi) + e_y^-(\omega, \theta, \phi)e_z^+(\omega, \theta, \phi)],$$

where e_p^+ and e_p^- with $p = (x, y, z)$ are the Cartesian coordinates of the unit electric field vectors e^+ and e^- corresponding to the refractive indices n^+ and n^- defined in Appendix A.

The unit electric field vectors \hat{e}^+ and \hat{e}^- are calculated from the propagation equation projected on the three axes of the optical frame. We obtain, for each wave, three equations that relate the three components (e_x, e_y, e_z) to the unit wave vector components (u_x, u_y, u_z):

$$(n^\pm)^2 [e_p^\pm - u_p(u_x e_x^\pm + u_y e_y^\pm + u_z e_z^\pm)] = (n_p)^2 e_p^\pm,$$

$$(p = x, y, z), \quad (e_x^\pm)^2 + (e_y^\pm)^2 + (e_z^\pm)^2 = 1.$$

The double refraction angle associated with the two eigenmodes can be calculated by

$$\rho^\pm(\omega) = \varepsilon \arccos[\hat{e}^\pm(\omega) \cdot \hat{u}(\omega)] - \varepsilon(\pi/2),$$

where ε is the sign of the direction of optical propagation $\hat{u}(\theta, \phi)$.

ACKNOWLEDGMENTS

This study is supported by the Délégation Générale pour l'Armement under contract 95-346 and by the Région Bourgogne under the 3ème Plan Etat-Région. We thank M. Jannin (Laboratoire de Physique de l' Université de Bourgogne) for the x-ray orientation of the sphere.

REFERENCES

1. F. C. Zumsteg, J. D. Bierlein, and T. E. Gier, "K_xRb_{1-x}TiOPO₄: a new nonlinear optical material," *J. Appl. Phys.* **47**, 4980-4985 (1976).
2. R. C. Eckardt, H. Masuda, Y. X. Fan, and R. L. Byer, "Absolute and relative nonlinear optical coefficients of KDP, KD*P, BaB₂O₄, LiIO₃, MgO:LiNbO₃ and KTP measured by phase-matched second harmonic generation," *IEEE J. Quantum Electron.* **26**, 922-933 (1990).
3. B. Boulanger, J. P. Fève, G. Marnier, B. Ménaert, X. Cabirol, P. Villeval, and C. Bonnin, "Relative sign and absolute magnitude of $d^{(2)}$ nonlinear coefficients of KTP from second-harmonic-generation measurements," *J. Opt. Soc. Am. B* **11**, 750-757 (1994).
4. E. C. Cheung, K. Koch, G. T. Moore, and J. M. Liu, "Measurement of second-order nonlinear optical coefficients from spectral brightness of parametric fluorescence," *Opt. Lett.* **19**, 168-170 (1994).
5. S. X. Dou, M. H. Jiang, Z. S. Shao, and X. T. Tao, "Maker fringes in biaxial crystals and the nonlinear optical coefficients of thiosemicarbazide cadmium chloride monohydrate," *Appl. Phys. Lett.* **54**, 1101-1103 (1989).
6. J. W. Perry, in *Materials for Nonlinear Optics, Chemical Perspectives*, S. R. Marder, J. E. Sohn, and G. D. Stucky, eds., ACS Symp. Ser. **455** (1991), Chap. 4.
7. R. C. Eckardt and R. L. Byer, "Measurement of nonlinear optical coefficients by phase-matched harmonic generation," in *Inorganic Crystals for Optics, Electro-Optics, and Frequency Conversion*, P. F. Bordui, ed., Proc. SPIE **1561**, 119-127 (1991).
8. S. P. Velsko, "Direct measurements of phase-matching properties in small crystals of new nonlinear materials," *Opt. Eng.* **28**, 76-84 (1989).
9. G. Marnier and B. Boulanger, "The sphere method: a new technique in linear and nonlinear crystalline optical studies," *Opt. Commun.* **72**, 139-143 (1989).
10. J. J. Zondy, "Comparative theory of walk-off limited type II versus type I second harmonic generation with Gaussian beams," *Opt. Commun.* **81**, 427-440 (1991).
11. J. J. Zondy, M. Abed, and A. Clairon, "Type II frequency doubling at $\lambda = 1.30 \mu\text{m}$ and $\lambda = 2.53 \mu\text{m}$ in flux-grown potassium titanyl phosphate," *J. Opt. Soc. Am. B* **11**, 2004-2015 (1994).
12. G. Marnier, "Process for the flux synthesis of crystals of the KTiOPO₄, potassium titanyl monophosphate type," U.S. patent 4,746,396 (May 24, 1988).
13. B. Boulanger, "Synthèse en flux et étude des propriétés optiques cristallines linéaires et non linéaires par la méthode de la sphère de KTiOPO₄ et des nouveaux composés isotypes et solutions solides de formule générale (K, Rb, Cs)TiO(P, As)O₄," Ph.D. dissertation (Université de Nancy I, Vandoeuvre-lès-Nancy, France, 1989).
14. J. P. Fève, "Existence et symétrie des interactions à 3 et 4 photons dans les cristaux anisotropes. Méthodes de mesure des paramètres affectant les couplages à 3 ondes: étude de KTP et isotypes," Ph.D. dissertation (Université de Nancy I, Vandoeuvre-lès-Nancy, France, 1994).
15. B. Boulanger, G. Marnier, B. Ménaert, X. Cabirol, J. P. Fève, C. Bonnin, and P. Villeval, "Collinear type II phase-matching for SHG in KTiOAsO₄: demonstration of its impossibility at 1.064 μm and first experiment at 1.32 μm . Comparison with KTiOPO₄," *Nonlin. Opt.* **4**, 133-142 (1993).
16. J. P. Fève, B. Boulanger, and G. Marnier, "Experimental study of internal and external conical refraction in KTP," *Opt. Commun.* **105**, 243-252 (1994).
17. J. P. Fève, B. Boulanger, X. Cabirol, B. Ménaert, G. Marnier, C. Bonnin, and P. Villeval, "Non-critically phase-matched cascaded THG at 440 nm in KTiOP_{1-y}As_yO₄ crystals," *Opt. Commun.* **115**, 323-326 (1994).
18. See, for example, A. Yariv and P. Yeh, *Optical Waves in Crystals* (Wiley, New York, 1984), Chap. 2, pp. 33-36.
19. J. P. Fève, B. Boulanger, and G. Marnier, "Experimental study of walk-off attenuation for type II second-harmonic-generation in KTP," *IEEE J. Quantum Electron.* **31**, 1569-1571 (1995).
20. J. P. Fève, B. Boulanger, and G. Marnier, "Determination of the longitudinal profile of a focused Nd:YAG Gaussian beam from second-harmonic-generation in a thin KTP crystal," *Appl. Opt.* **33**, 3169-3174 (1994).
21. K. Kato, "Parametric oscillation at 3.2 μm in KTP pumped at 1.064 μm ," *IEEE J. Quantum Electron.* **27**, 1137-1140 (1991).
22. S. C. Mehendale and P. K. Gupta, "Effect of double refraction on type II phase-matched second harmonic generation," *Opt. Commun.* **68**, 301-304 (1988).
23. B. Boulanger and G. Marnier, "Field factor calculation for the study of the relationships between all the 3-wave nonlinear optical interactions in uniaxial and biaxial crystals," *J. Phys. Condens. Matter* **3**, 8327-8350 (1991).